Supporting Information

A Water-Soluble Copper-Immobilized Covalent Organic Framework Functioning as an "OFF–ON" Fluorescent Sensor for Amino Acids

Lamiaa Reda Ahmed,[a] Ahmed F. M. EL-Mahdy,[b] Cheng-Tang Pan,[a,c] and Shiao-Wei Kuo*[b,d]

[a]*Institute of Medical Science and Technology, National Sun Yat-Sen University, Kaohsiung 80424, Taiwan.*

[b]*Department of Materials and Optoelectronic Science, National Sun Yat-Sen University, Kaohsiung 80424, Taiwan.*

[c]*Department of Mechanical and Electro-Mechanical Engineering, National Sun Yat-Sen University, Kaohsiung 80424, Taiwan.*

[d]*Department of Medicinal and Applied Chemistry, Kaohsiung Medical University, Kaohsiung 807, Taiwan.*

Corresponding authors:
Shiao-Wei Kuo, +886-7-5252000 ext 4079, E-mail: kuosw@faculty.nsysu.edu.tw

Section	Content	Page No.
S1	Characterization	S3
S2	Synthetic Procedures	S4
S3	Spectral Profiles of Monomers	S5
S4	PXRD data and BET parameters	S8
S5	Structural Modeling and Fractional Atomic Coordinates for COF Structure	S8
S6	Field Emission Scanning Electron Microscopy (FE-SEM)	S12
S7	Transmission Electron Microscopy (TEM)	S12
S8	Thermal Gravimetric Analysis	S13
S9	Chemical Stability of the TFPB-DHTH COF	S13
S10	Photophyscial Properties of TFPB-DHTH COF	S15
S11	X-Ray photoelectron spectroscopy (XPS) analysis	S16
S12	“OFF-ON” Fluorescence Detection Assay	S17
S13	References	S20

S1. Characterization

^{1}H and ^{13}C NMR spectroscopy. NMR spectra were recorded using an INOVA 500 instrument with DMSO-d_6 and $CDCl_3$ as solvents and tetramethylsilane (TMS) as the external standard. Chemical shifts are provided in parts per million (ppm).

Fourier-transform infrared spectroscopy (FRIR) spectroscopy. FTIR spectra were recorded using a Bruker Tensor 27 FTIR spectrophotometer and the conventional KBr plate method; 32 scans were collected at a resolution of 4 cm^{-1}.

Solid state nuclear magnetic resonance (SSNMR) spectroscopy. SSNMR spectra were recorded using a a Brukerb avance III HD Solid State NMR spectrometer in National Cheng Kung University and a Bruker magic-angle-spinning (MAS) probe, running 32,000 scans.

Thermogravimetric analysis (TGA). TGA was performed using a TA Q-50 analyzer under a flow of N_2. The samples were sealed in a Pt cell and heated from 40 to 800 °C at a heating rate of 20 °C min^{-1} under N_2 at a flow rate of 50 mL min^{-1}.

Powder X-Ray Diffraction (PXRD). PXRD was performed using a Siemens D5000 and monochromated $Cu/K\alpha$ ($\lambda = 0.1542\ nm$). The sample was spread in a thin layer on the square recess of an XRD sample holder.

Surface area and porosimetry (ASAP/BET). The BET surface areas and porosimetry measurements of the prepared samples (ca. 20–100 mg) were performed using a Micromeritics ASAP 2020 Surface Area and Porosity analyzer. Nitrogen isotherms were generated through incremental exposure to ultrahigh-purity N_2 (up to ca. 1 atm) in a liquid N_2 (77 K) bath.

COF structural simulations. Molecular modeling was performed using Reflex, a software package for crystal determination from XRD patterns. Unit cell dimensions were first determined manually from the observed XRD peak positions using the coordinates.

S2. Synthetic Procedures

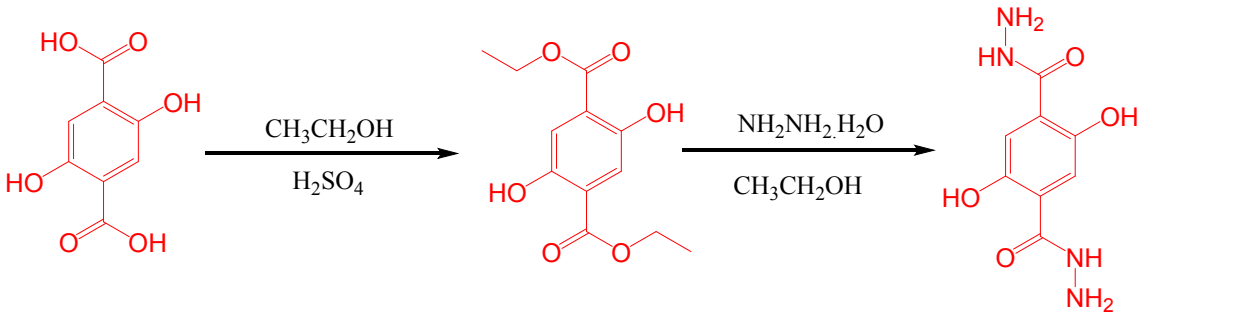

2,5-dihydroxyterephthalohydrazide
(**DHTH**)

Scheme S1. Synthesis of 2,5-dihydroxyterephthalohydrazide (DHTH).

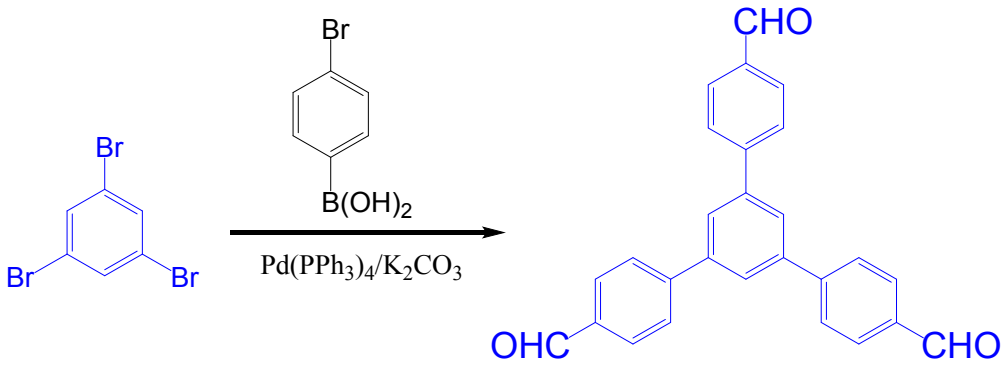

1,3,5-tris(4-formylphenyl)benzene
(**TFPB-3CHO**)

Scheme S2. Synthesis of 1,3,5-tris(4-formylphenyl)benzene (TFPB-3CHO).

S3. Spectral Profiles of monomers

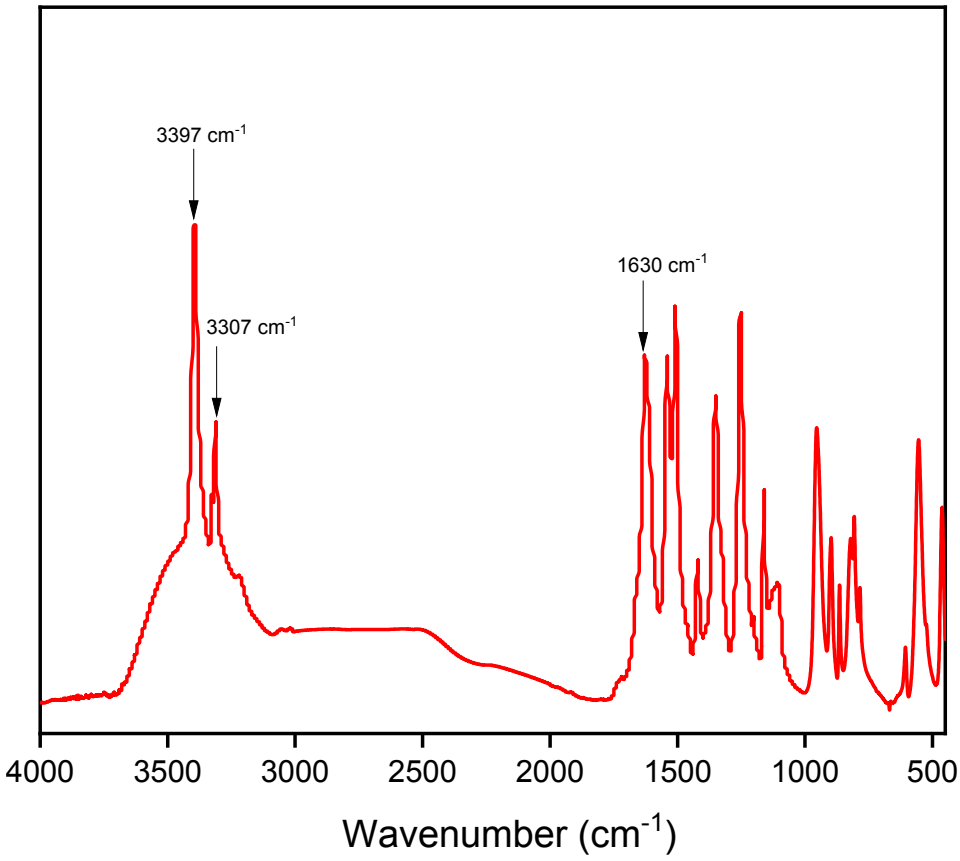

Figure S1. FT-IR spectrum of 2,5-dihydroxyterephthalohydrazide (DHTH).

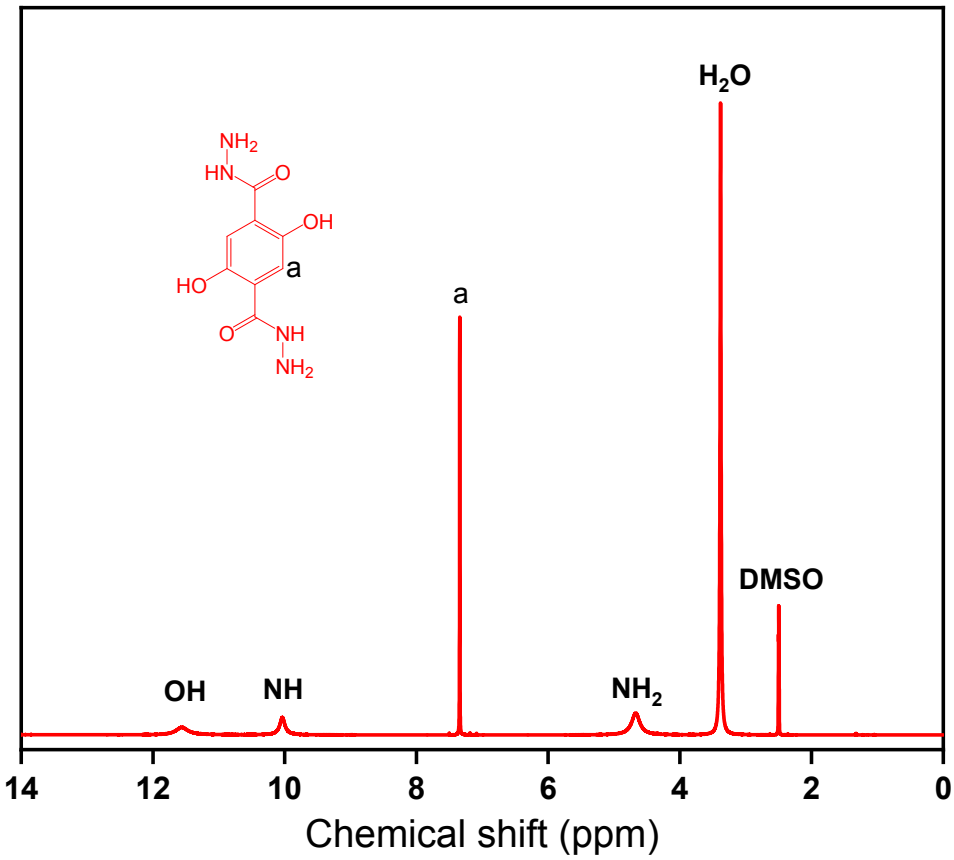

Figure S2. [1]H NMR spectrum of 2,5-dihydroxyterephthalohydrazide (DHTH).

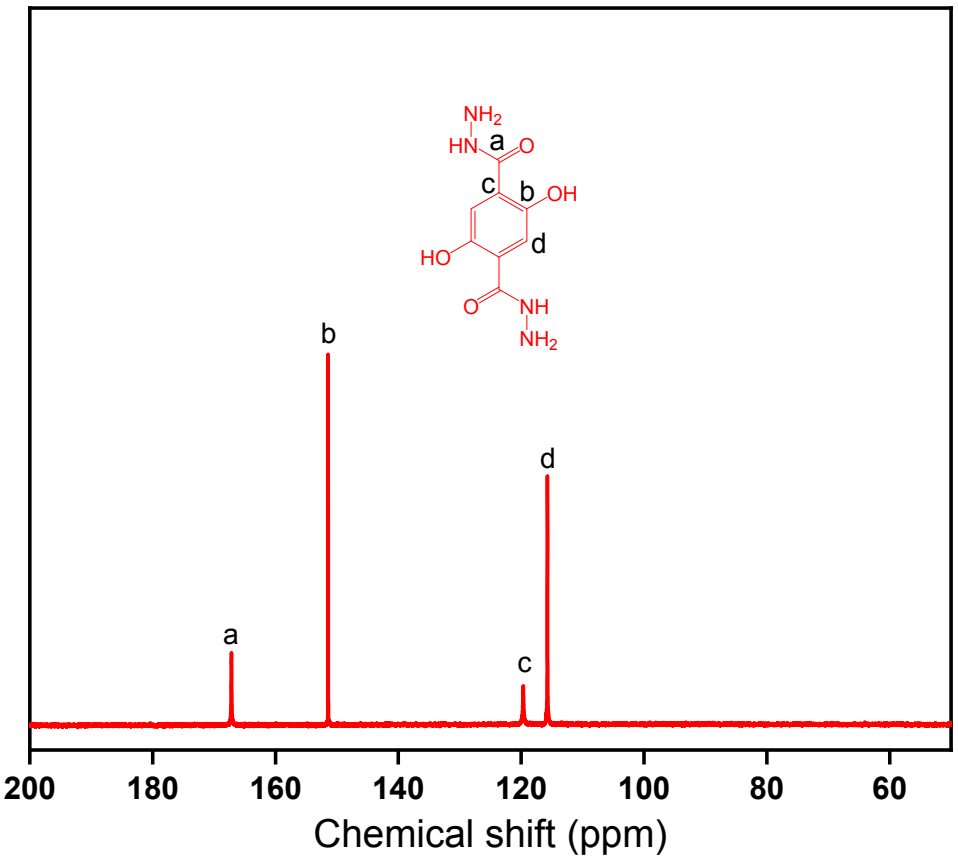

Figure S3. ^{13}C NMR spectrum of 2,5-dihydroxyterephthalohydrazide (DHTH).

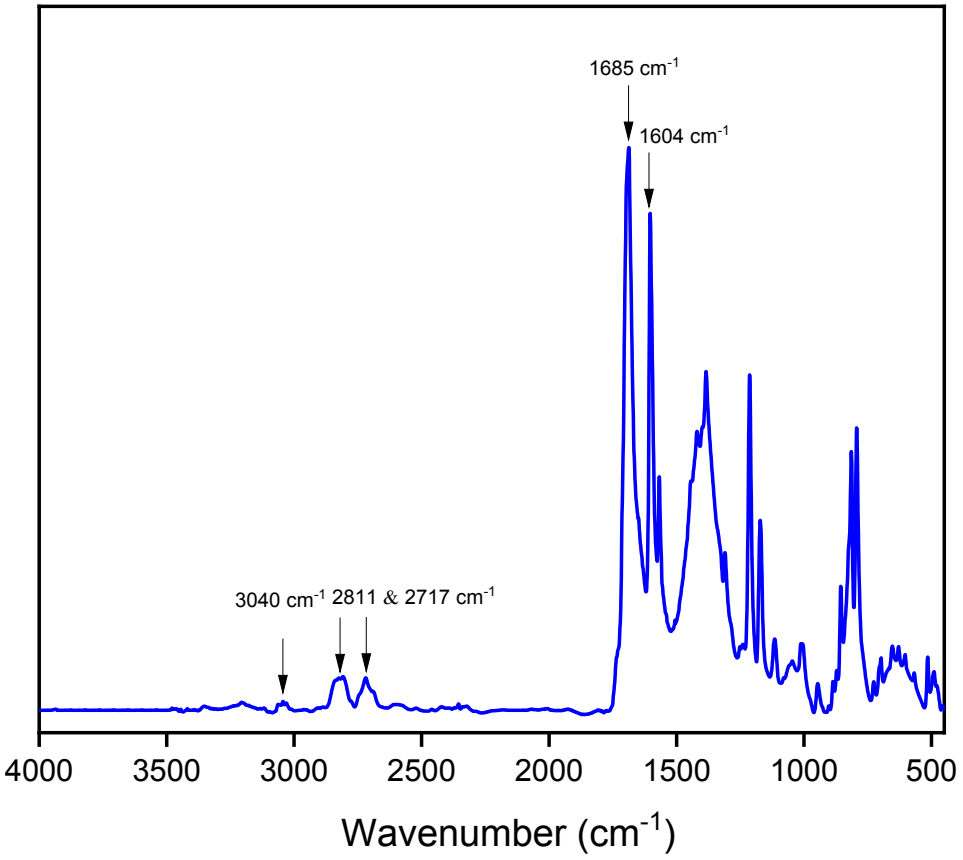

Figure S4. FT-IR spectrum of 1,3,5-tris(4-formylphenyl)benzene (TFPB-3CHO).

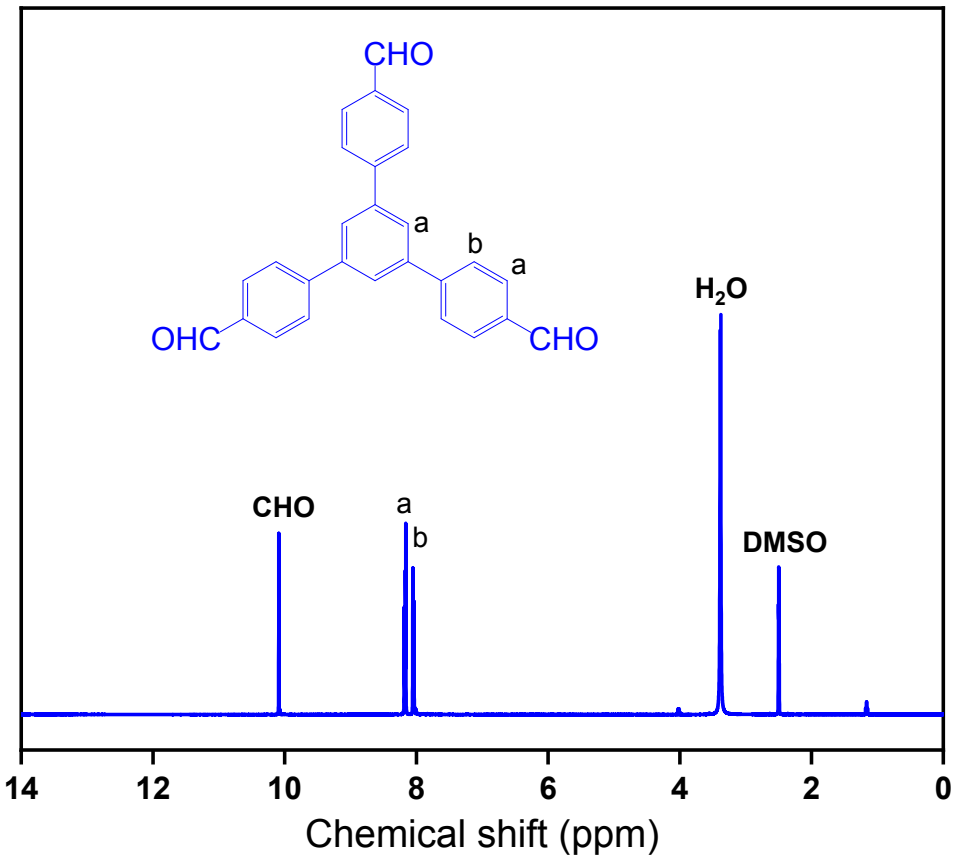

Figure S5. ^{1}H NMR spectrum of 1,3,5-tris(4-formylphenyl)benzene (TFPB-3CHO).

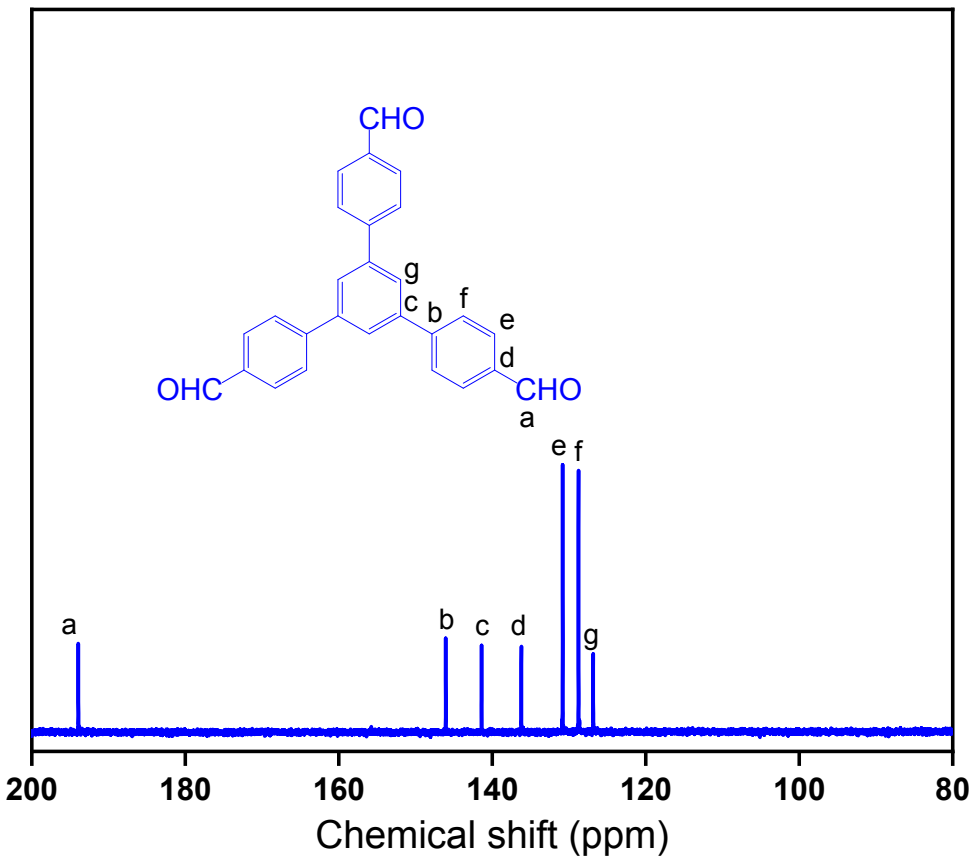

Figure S6. ^{13}C NMR spectrum of 1,3,5-tris(4-formylphenyl)benzene (TFPB-3CHO).

S4. PXRD data and BET parameters

Table S1. PXRD and BET parameters of the synthesized COFs.

COF	S_{BET} ($m^2\ g^{-1}$)	d_{100} (nm)	Pore size (nm)	Pore volume ($cm^3\ g^{-1}$)	Interlayer Distance (Å)
TFPB-DHTH	360	4.01	3.77	0.58	3.45

S5. Structural Modeling and Fractional Atomic Coordinates for COF Structure

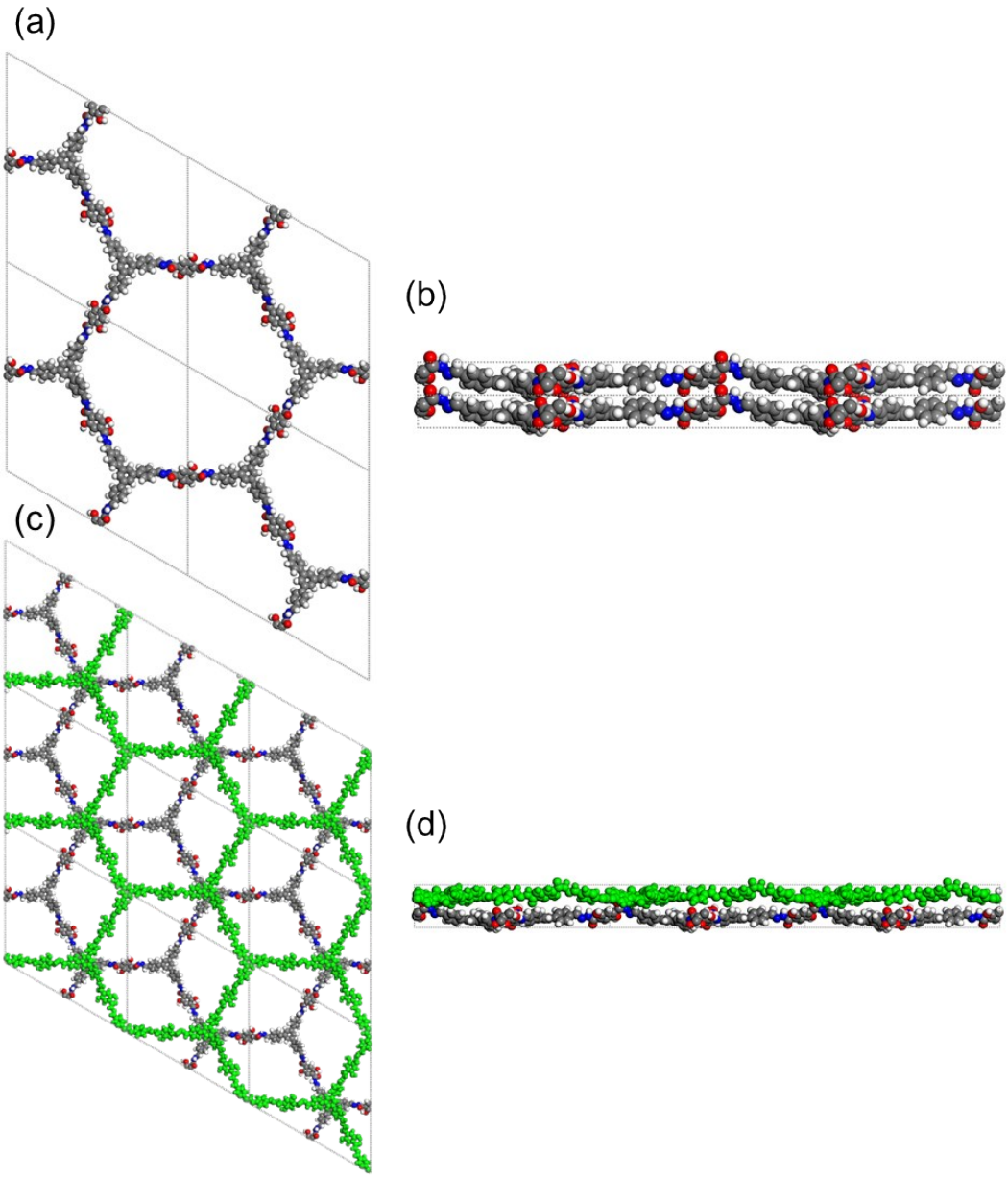

Figure S7. Crystalline structure for the TFPB-DHTH COF (a, b) completely eclipsed AA-stacking models and (c, d) staggered AB-stacking successions models.

Table S2. Fractional atomic coordinates for the unit cell of the TFPB-DHTH COF with eclipsed AA-stacking model.

Sample Name : TFPB-DHTH COF							
Space Group : P 1							
a = 46.23100 , b = 46.23100, c = 4.07851 $\alpha = \beta = 90°, \gamma = 120°$							
R_{wp}= 4.91% R_p= 3.72%							
Atom	*x/a*	*y/b*	*z/c*	Atom	*x/a*	*y/b*	*z/c*
C1	0.60426	0.16673	0.5738	C30	0.46226	0.45959	0.25054
C2	0.63673	0.19111	0.65973	C31	0.48424	0.44661	0.26022
C3	0.65015	0.22492	0.58724	C32	0.51808	0.46671	0.34016
C4	0.63177	0.23618	0.42363	C33	0.52917	0.50025	0.42553
C5	0.59947	0.21165	0.32712	C34	0.50722	0.51309	0.4148
C6	0.58584	0.17733	0.40141	C35	0.3656	0.59073	0.29195
C7	0.64626	0.27342	0.37002	C36	0.3855	0.57542	0.31643
C8	0.68111	0.29453	0.33079	C37	0.41322	0.58845	0.50815
C9	0.69591	0.32958	0.30566	C38	0.42057	0.61732	0.67092
C10	0.67483	0.34363	0.31535	C39	0.40109	0.63278	0.6441
C11	0.63981	0.32357	0.35304	C40	0.37315	0.6198	0.45534
C12	0.62599	0.2884	0.37741	C41	0.39172	0.74692	0.30685
C13	0.73343	0.35151	0.27487	C42	0.40689	0.782	0.34308
C14	0.75573	0.34509	0.4376	C43	0.39395	0.79577	0.54594
C15	0.7907	0.36565	0.4086	C44	0.36507	0.77355	0.70481
C16	0.80453	0.39298	0.21231	C45	0.34959	0.73876	0.66409
C17	0.78231	0.39921	0.04827	C46	0.36282	0.72468	0.46771
C18	0.74743	0.37907	0.08071	C47	0.31649	0.61655	0.4326
C19	0.61798	0.33947	0.38123	C48	0.35178	0.63618	0.43683
C20	0.62477	0.36861	0.22251	C49	0.36648	0.67142	0.43972
C21	0.60444	0.38338	0.2541	C50	0.34683	0.68705	0.44126
C22	0.57668	0.36946	0.44562	C51	0.31162	0.66652	0.43353
C23	0.57005	0.34051	0.60386	C52	0.29576	0.63115	0.43066
C24	0.59028	0.3259	0.57316	C53	0.2065	0.55569	0.34482
C25	0.43456	0.5726	0.55288	C54	0.24137	0.5767	0.31905
C26	0.55389	0.38371	0.48768	C55	0.25777	0.60946	0.43623
C27	0.54222	0.45405	0.30016	C56	0.2373	0.62071	0.56695
C28	0.45136	0.50836	0.27167	C57	0.20225	0.59995	0.58412
C29	0.4737	0.49345	0.32085	C58	0.18643	0.56694	0.47801

Continuous (**Table S3**)

Atom	*x/a*	*y/b*	*z/c*	Atom	*x/a*	*y/b*	*z/c*
C59	0.15043	0.54272	0.54611	O94	0.55116	0.04217	1.12888
C60	0.06628	0.50066	0.51526	O95	0.03054	0.53167	0.8047
C61	0.01017	0.45985	0.31285	O96	0.42899	0.43868	0.171
C62	0.02951	0.48861	0.48527	O97	0.5616	0.52172	0.52563
C63	0.01257	0.50192	0.64602	O98	0.48433	0.03746	0.53628
C64	0.58939	0.13348	0.72852	O99	0.43866	0.91378	0.14689
C65	0.54364	0.04903	0.89174	O100	0.51578	0.93492	0.64883
C66	0.52993	-0.00736	0.71674	H101	0.90904	0.42221	0.75111
C67	0.52255	0.01895	0.7001	H102	0.9588	0.41405	0.14448
C68	0.49296	0.01246	0.55459	H103	0.65146	0.18419	0.79835
C69	0.41183	0.83225	0.62778	H104	0.67461	0.24256	0.67369
C70	0.45369	0.91791	0.37901	H105	0.58451	0.21903	0.19805
C71	0.47773	0.9531	0.48059	H106	0.56043	0.15948	0.33756
C72	0.5079	0.96027	0.61426	H107	0.69703	0.28362	0.31656
C73	0.47116	0.97982	0.4405	H108	0.68601	0.37053	0.30609
C74	0.84161	0.41458	0.16635	H109	0.59939	0.27263	0.4097
C75	0.92055	0.43616	0.51981	H110	0.74614	0.32445	0.59198
C76	0.95789	0.45566	0.48071	H111	0.80705	0.36	0.53742
C77	0.9751	0.44328	0.3108	H112	0.792	0.4197	-0.10777
C78	0.97717	0.48524	0.64455	H113	0.73131	0.38453	-0.05292
N79	0.4328	0.54845	0.3887	H114	0.64543	0.37968	0.06852
N80	0.45352	0.53428	0.44079	H115	0.61017	0.40549	0.12673
N81	0.55825	0.41109	0.36125	H116	0.5492	0.32924	0.75627
N82	0.5358	0.42335	0.40717	H117	0.58452	0.30425	0.70698
N83	0.1262	0.55042	0.52049	H118	0.45268	0.58221	0.73097
N84	0.0927	0.52953	0.6487	H119	0.53272	0.37037	0.63409
N85	0.56254	0.10523	0.65474	H120	0.46983	0.54245	0.6207
N86	0.54717	0.08052	0.87915	H121	0.5142	0.40946	0.53338
N87	0.42914	0.85674	0.44291	H122	0.47512	0.42105	0.19282
N88	0.44784	0.89038	0.54431	H123	0.51697	0.53908	0.47151
N89	0.86352	0.41531	0.35348	H124	0.34458	0.5801	0.14152
N90	0.89872	0.43529	0.31457	H125	0.37926	0.55335	0.18661
N91	0.43148	0.49789	0.06753	H126	0.44147	0.62788	0.82297
O92	0.56789	0.47115	0.16181	H127	0.40742	0.65453	0.7785
O93	0.07811	0.51141	0.76167	H128	0.40253	0.73711	0.1519

Continuous (**Table S3**)

Atom	*x/a*	*y/b*	*z/c*	Atom	*x/a*	*y/b*	*z/c*
H129	0.42937	0.79829	0.22056	H143	0.5549	0.09004	1.09248
H130	0.35479	0.78315	0.86767	H144	0.55265	-0.00281	0.82681
H131	0.32789	0.72271	0.79647	H145	0.01616	0.53844	0.92055
H132	0.30524	0.5897	0.44415	H146	0.42304	0.41522	0.11419
H133	0.39339	0.68685	0.4464	H147	0.57586	0.51118	0.5624
H134	0.29659	0.67843	0.42586	H148	0.46269	0.0298	0.42389
H135	0.19516	0.53031	0.26262	H149	0.40929	0.83837	0.85458
H136	0.25547	0.56697	0.20857	H150	0.45842	0.89514	0.75488
H137	0.24835	0.64516	0.6676	H151	0.44842	0.97464	0.32881
H138	0.18766	0.60907	0.69633	H152	0.53849	0.94318	0.74377
H139	0.14444	0.51884	0.64124	H153	0.8503	0.43044	-0.02783
H140	0.10755	0.55107	0.50868	H154	0.90968	0.44937	0.12957
H141	0.02228	0.44895	0.18691	H155	0.96457	0.49485	0.77931
H142	0.60098	0.13456	0.93938	H156	0.93344	0.40241	0.14459

S6. Field Emission Scanning Electron Microscopy (FE-SEM)

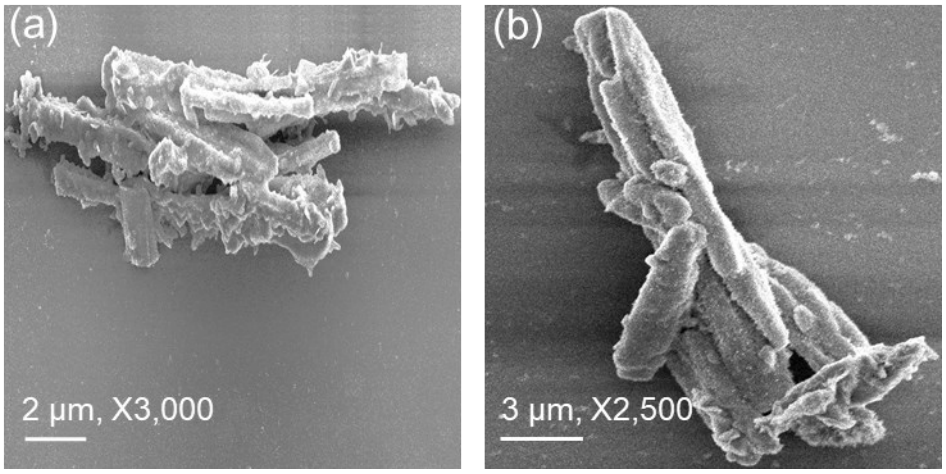

Figure S8. FE-SEM images of the TFPB-DHTH COF at different magnification scales: (a) 2 µm, X3,000 and (b) 3 µm, X2,500.

S7. Transmission Electron Microscopy (TEM)

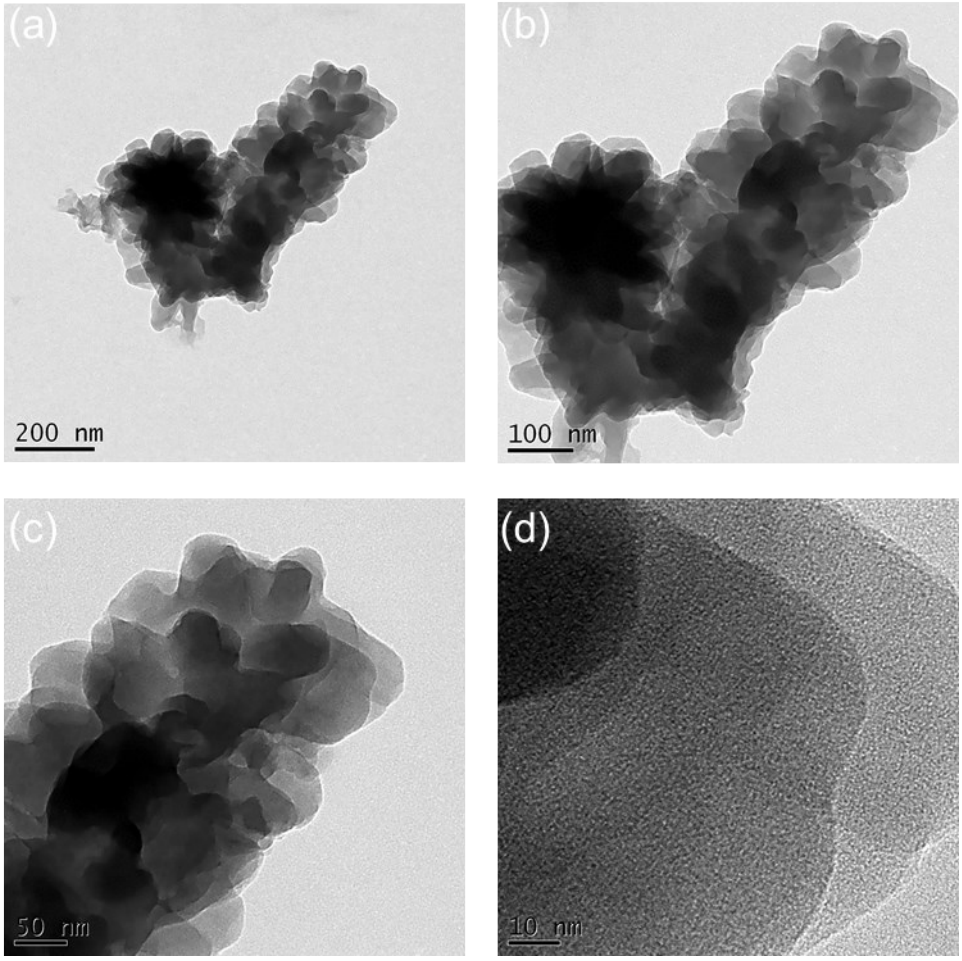

Figure S9. TEM images of the TFPB-DHTH COF different magnification scales: (a) 200 nm, (b) 100 nm, (c) 50 nm, and (d) 10 nm.

S8. Thermal Gravimetric Analysis

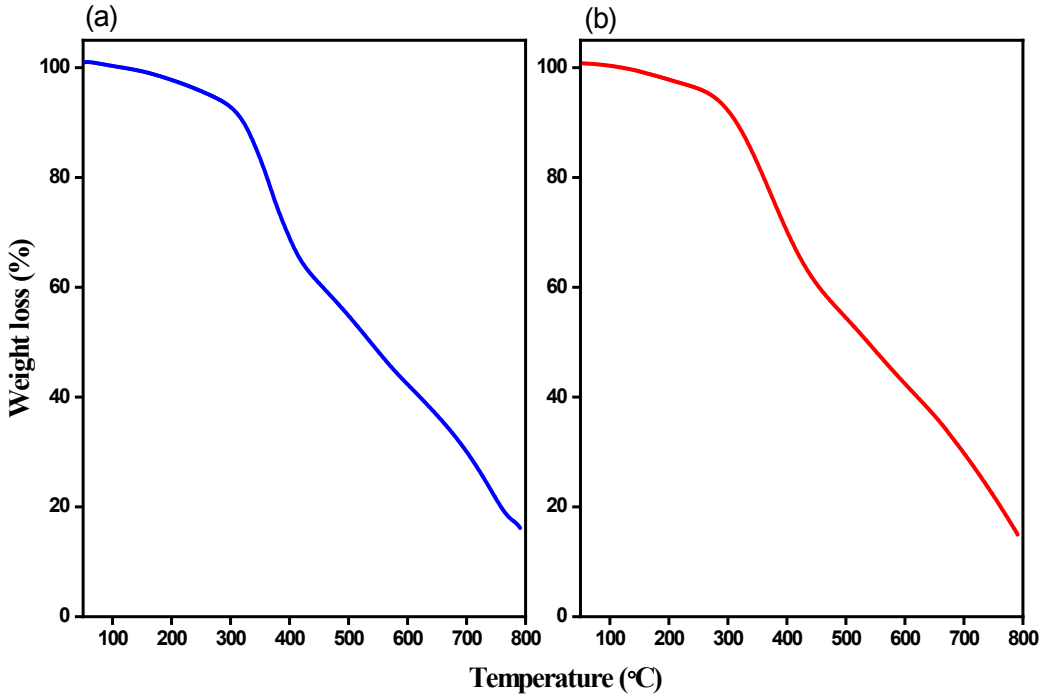

Figure S10. Thermogravimetric analysis trace of the TFPB-DHTH COF under (a) nitrogen and (b) air atmospheres with heating rate of 20°C min^{-1}.

S9. Chemical Stability of the TFPB-DHTH COF

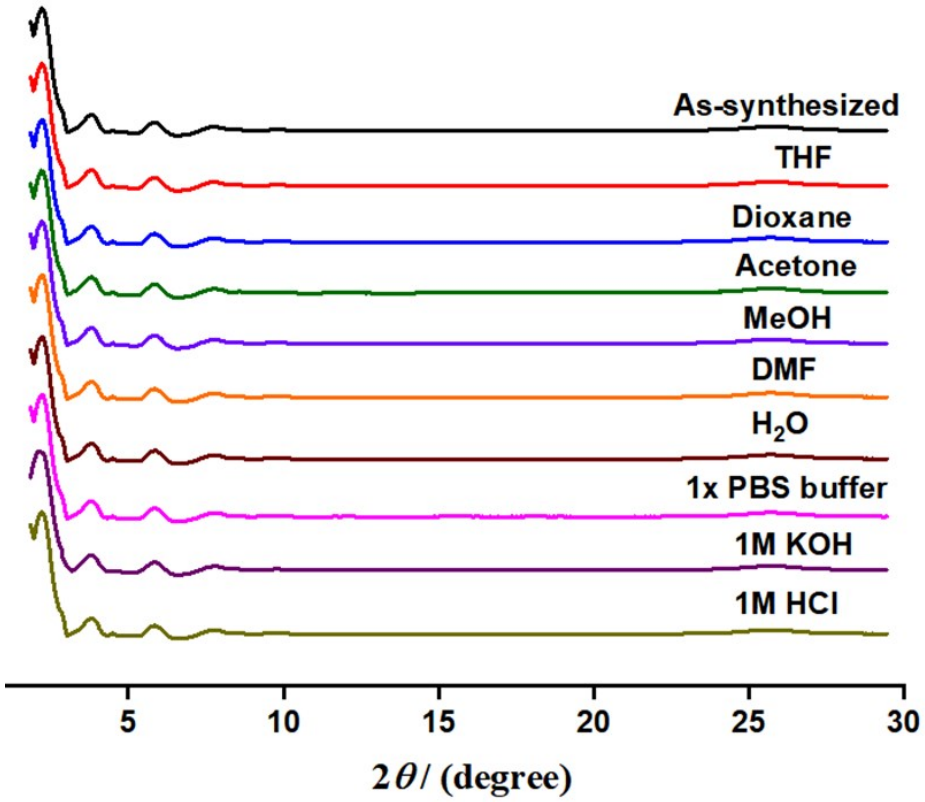

Figure S11. PXRD patterns of the TFPB-DHTH COF as-synthesized and after immersing 2 days in various solvents.

TableS3. BET surface areas of the TFPB-DHTH COF as-synthesized and after immersing 2 days in various solvents.

TFPB-DHTH COF	S_{BET} ($m^2\ g^{-1}$)
As-synthesized	360
THF	358
Acetone	355
DMF	340
H_2O	360
1x PBS buffer	259
1M KOH	335
1M HCl	332

S10. Photophyscial Properties of TFPB-DHTH COF

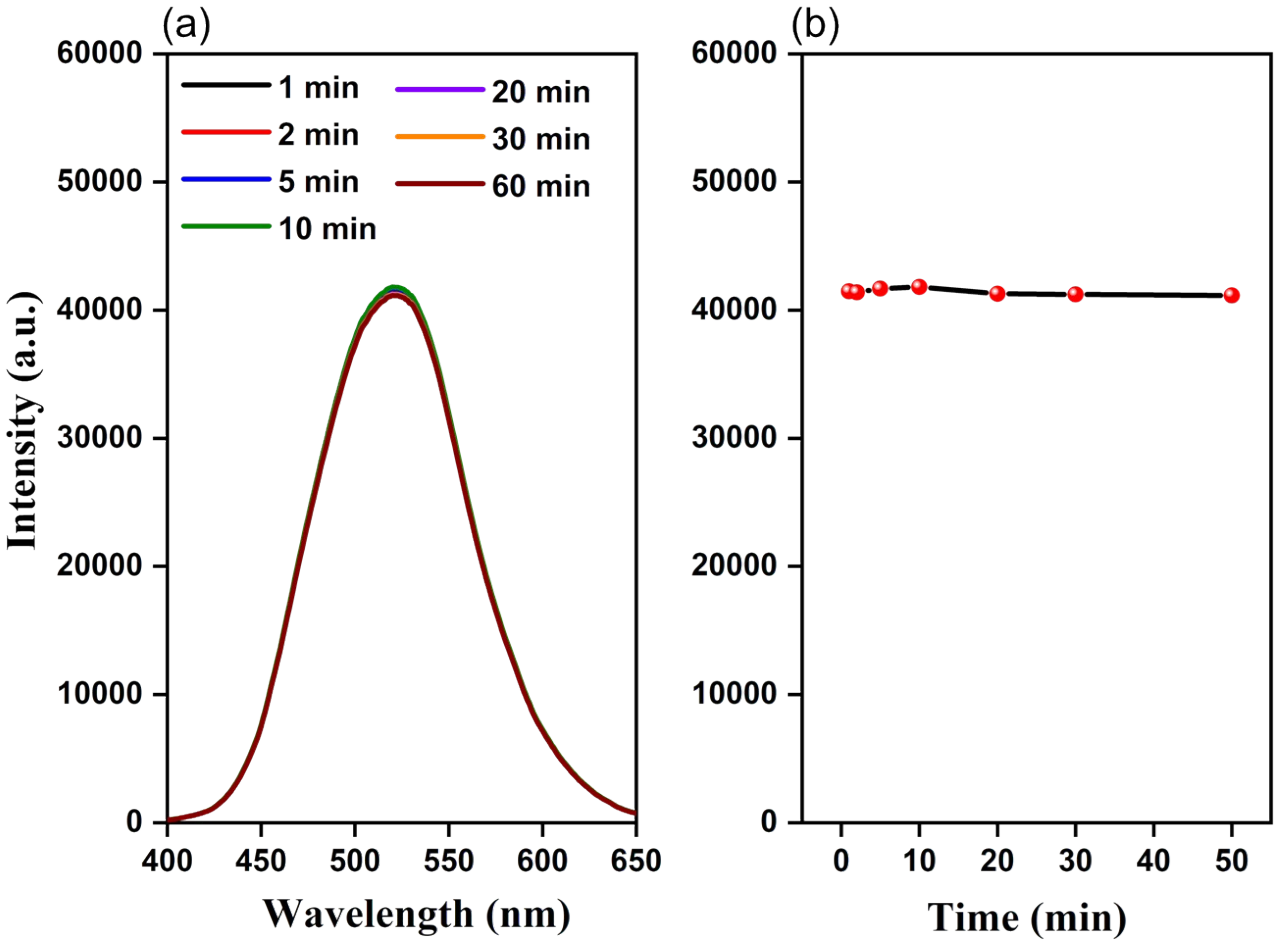

Figure S12. (a) Time-dependent fluorescence emission spectra and (b) Time-dependent fluorescence emission intensities at wavelength of 520 nm of the TFPB-DHTH COF dissolved in water within 60 mins (excitation at 365 nm).

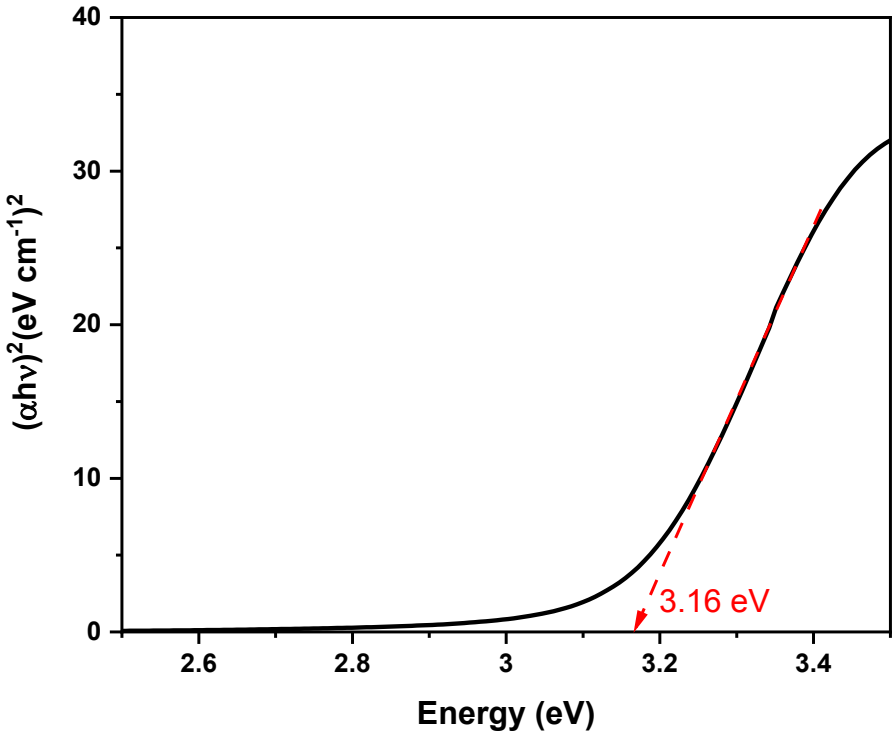

Figure S13. Bandgaps of TFPB-DHTH COF calculated by Tauc-plot.

S11. X-Ray photoelectron spectroscopy (XPS) analysis

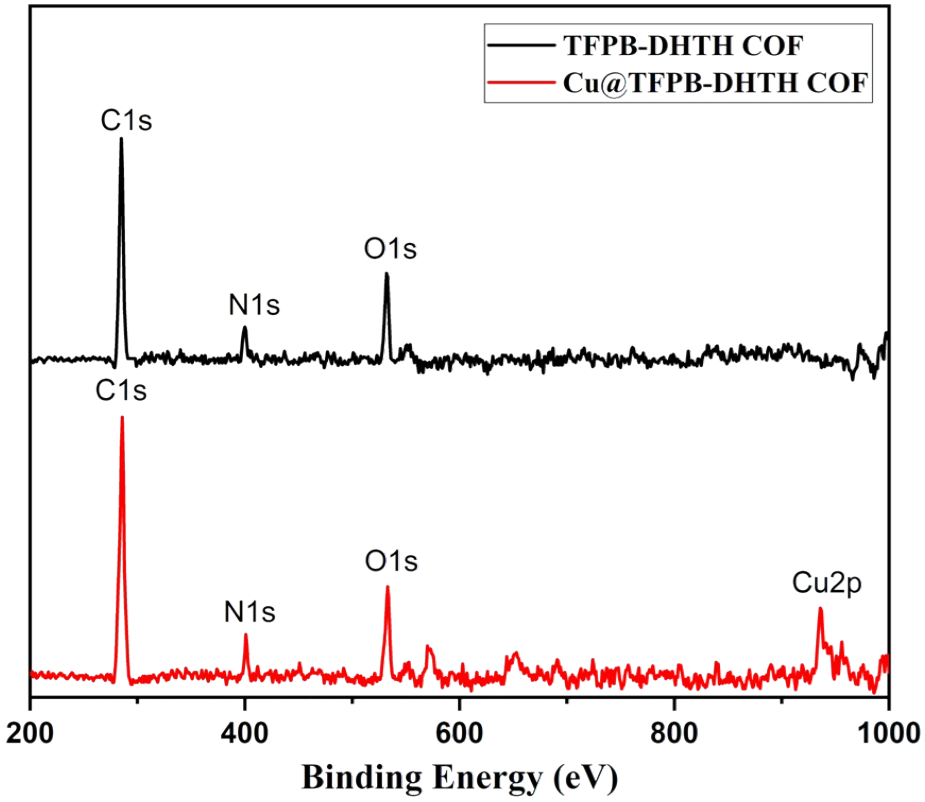

Figure S14. XPS spectra of TFPB-DHTH and Cu@TFPB-DHTH COFs.

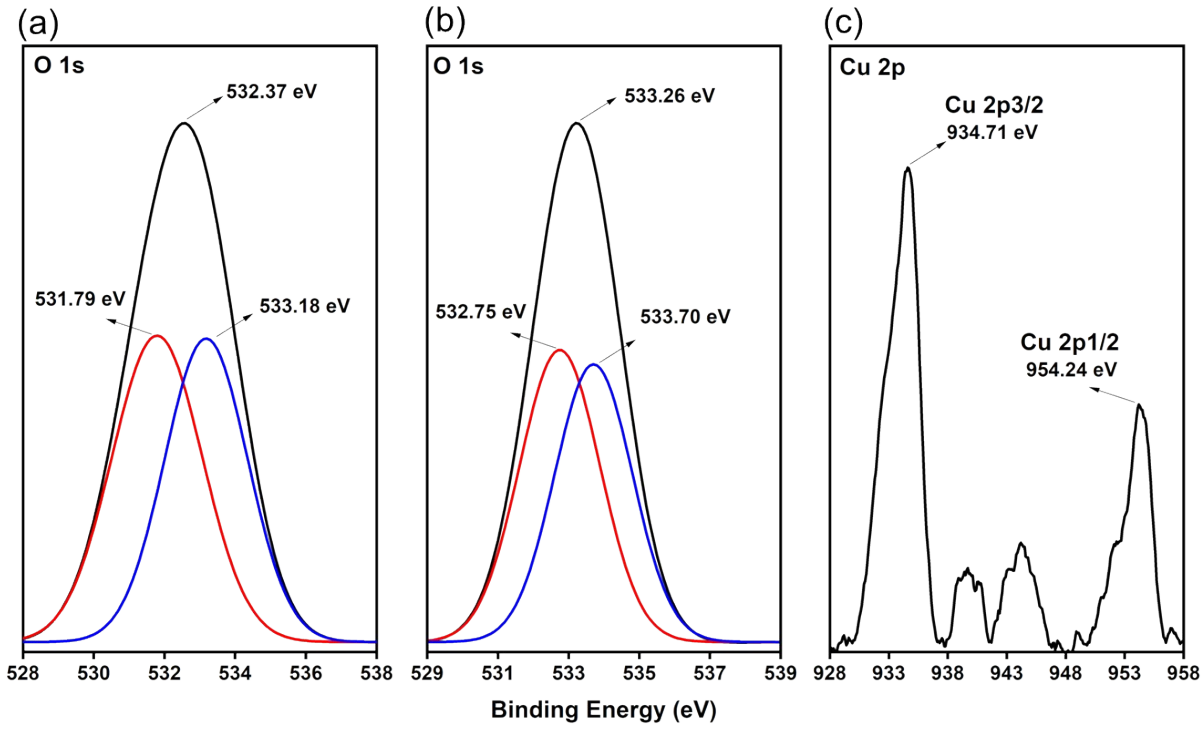

Figure S15. O 1s XPS spectra of (a) TFPB-DHTH and (b) Cu@TFPB-DHTH COFs. Cu 2p XPS spectrum of (c) Cu@TFPB-DHTH COF.

S12. "OFF-ON" Fluorescence Detection Assay

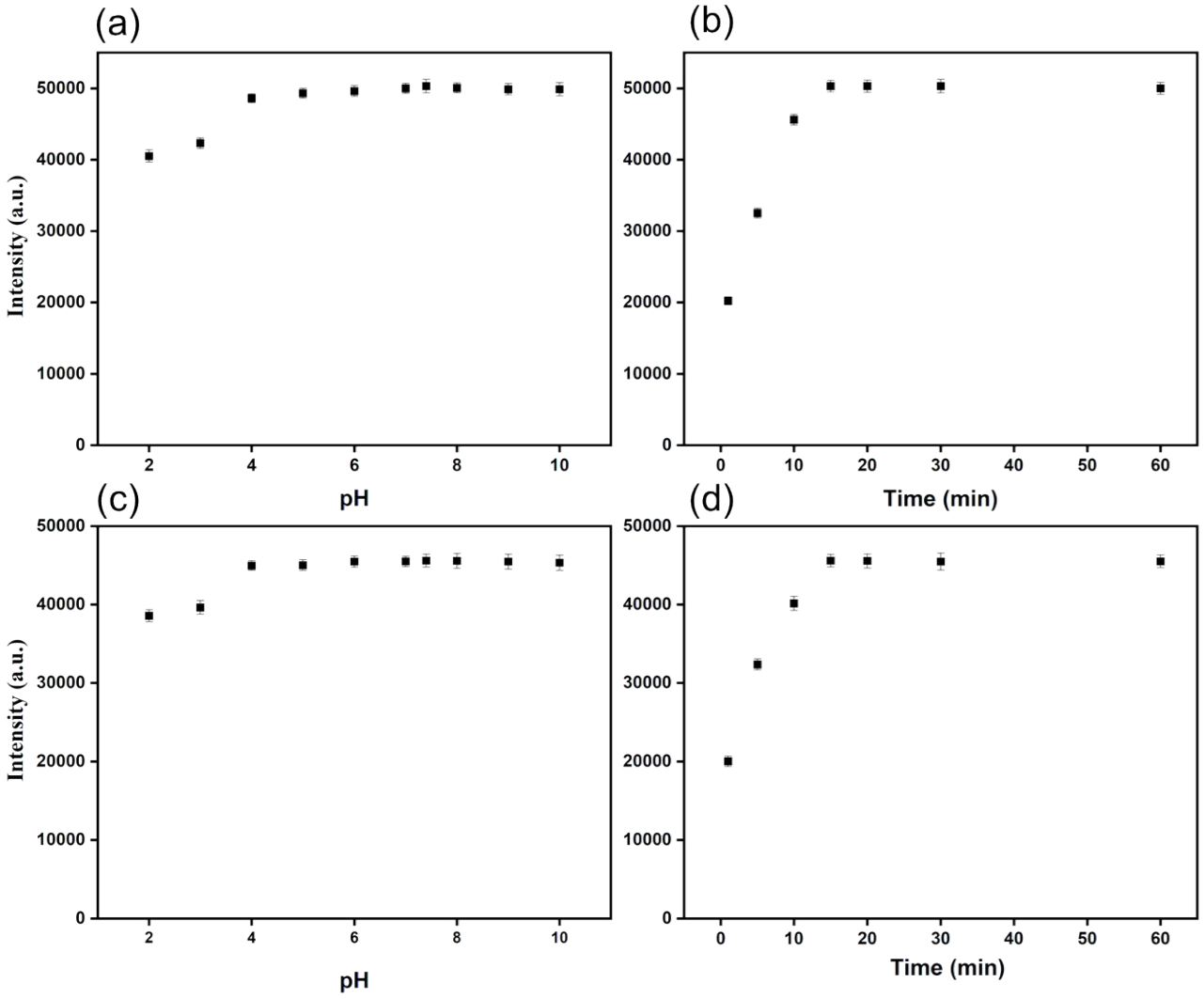

Figure S16. The effect of (a, c) pH and (b, d) time on the fluorescence recovery of the emission peak at wavelength of 520 nm in the presence of (a, b) cysteine (400 μM) or (c, d) L-histidine (500 μM).

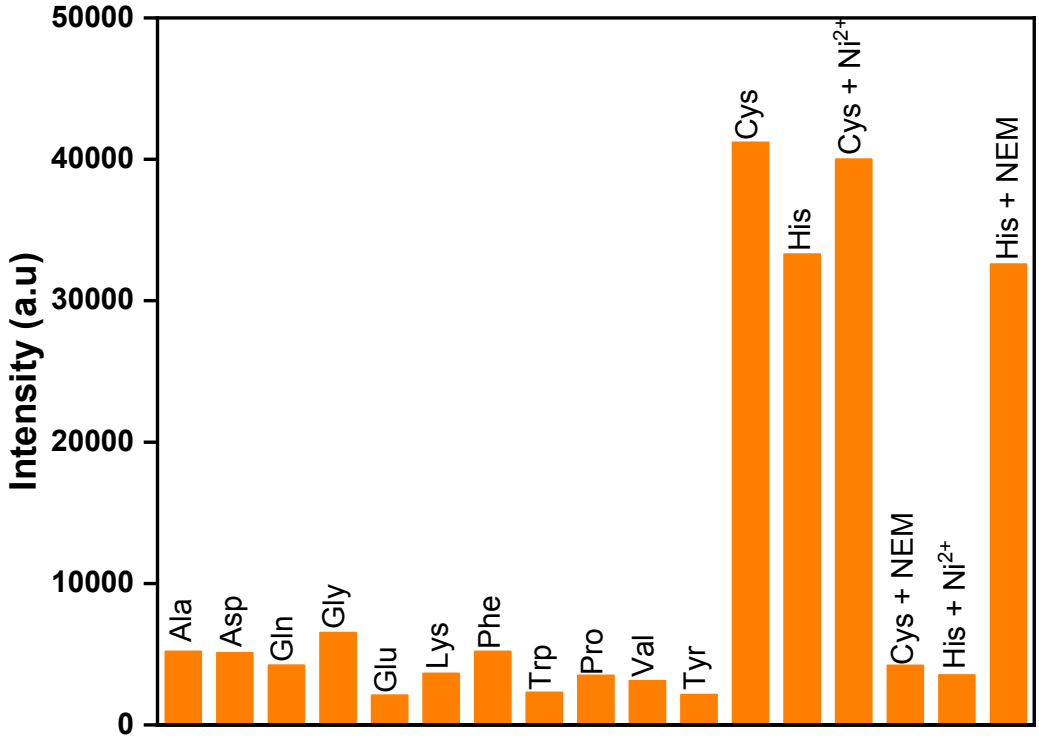

Figure S17. Fluorescence emission intensities at wavelength of 520 nm of the Cu@TFPB-DHTH COF dissolved in 1X PBS buffer (pH = 7.4) in the presence of cysteine, histidine and other amino acids. Measurements were carried out at a Cu@TFPB-DHTH COF concentration of 0.125 mg mL-1 COF and 200 μM Cu^{2+} ion and a concentration of amino acid of 200 μM under excitation at 365 nm.

Table S4. Comparison of detection limit with previously reported methods for cysteine and L-histidine.

	Probe	Limit of detection	Ref.
Cysteine			
	Organic molecule	460 nM	S1
	Organic molecule	874 nM	S2
	Organic molecule	8400 nM	S3
	DPAS-Cys	2400 nM	S4
	FSD-103-Cu^{2+}	200 nM	S5
	AgAuNCs@11-MUA-Cu^{2+}	111 nM	S6
L-histidine	Cu@TFPB-DHTH COF	340 nM	**This work**
	AgAuNCs@11-MUA-Cu^{2+}	87 nM	S6
	Ni^{2+}-modulated Hcy-capped CdTe QDs	200 nM	S7
	$[Cu(LH_2)Cl_2]\cdot 2H_2O$	1890 nM	S8
	EPANS-based probe	1000 nM	S9
	Chiral carbazole with urea-carboxylic acid moiety (CCS)	7640 nM	S10
	ruthenium(II) tris(bipyridine) derivative (Ru-DPA)	1380	S11
	Cu@TFPB-DHTH COF	520 nM	**This work**

S13. Reference

[S1] Y. Yue, F. Huo, P. Ning, Y. Zhang, J. Chao, X. Meng and C. Yin, *J. Am. Chem. Soc.*, 2017, **8**, 3181−3185.

[S2] C. Chen, W. Liu, C. Xu and W. Liu, *Biosens. Bioelectron.*, 2016, **85**, 46−52.

[S3] L. Bu, J. Chen, X. Wei, X. Li, H. Ågren and Y. Xie, *Dyes Pigm.*, 2017, **136**, 724−731.

[S4] W. Cheng, X. Xue, F. Zhang, B. Zhang, T. Li, L. Peng, D. H. Cho, H. Chen, J. Fang, and X. Chen, *Analytica Chimica Acta*, 2020, **1127**, 20−28.

[S5] Y. Caia, J. Fang, H. Zhu, W. Qin, Y. Cao, H. Yu, G. Shao, Y. Liu, and W. Liu, Sens. *Actuators B-Chem.*, 2020, **303**, 127214.

[S6] J. Sun, F. Yang, D. Zhao, C. Chen, and X. Yang, *ACS Appl. Mater. Interfaces*, 2015, 7, 6860−6866.

[S7] P. Wu, and X. -P. Yan, *Biosens. Bioelectron.*, 2010, **26**, 485−490.

[S8] C. Das, B. Pakhira, A. L. Rheingold, and S. K. Chattopadhyay, *Inorganica Chim. Acta*, 2018, **482**, 292–298.

[S9] X. Li, H. Ma, L. Nie, M. Sun, and S. Xiong, *Anal. Chim. Acta*, 2004, **515**, 255–260.

[S10] A. Pundi, C. J. Chang, J. Chen, S. R. Hsieh, and M. C. Lee, Sens. *Actuators B-Chem.*, 2021, **328**, 129084.

[S11] Y. Yang, Y. Li, X. Zhi, Y. Xu, and M. Li, *Dyes Pigm.*, 2020, **183**, 108690.